ATMOSPHERIC AND OCEANIC SCIENCE LETTERS, 2008, VOL. 1, NO. 1, 1–6

Causes of the Intraseasonal SST Variability in the Tropical Indian Ocean

Tim Li[1], Francis Tam[1], Xiouhua Fu[1], ZHOU Tian-Jun [2], ZHU Wei-Jun [3]

[1] *IPRC and Department of Meteorology, University of Hawaii at Manoa, Honolulu, Hawaii, USA*
[2] *Institute of Atmospheric Physics, Chinese Academy of Sciences, Beijing 100029, China*
[3] *Joint Climate Institute of CMA & NUIST, Nanjing University of Information Science & Technology, Nanjing 210044, China*

Received 16 May 2008; revised 11 June 2008; accepted 23 June 2008; published ***

Abstract Satellite observations reveal a much stronger intraseasonal sea surface temperature (SST) variability in the southern Indian Ocean along 5–10°S in boreal winter than in boreal summer. The cause of this seasonal dependence is studied using a 2½-layer ocean model forced by ERA-40 reanalysis products during 1987–2001. The simulated winter–summer asymmetry of the SST variability is consistent with the observed. A mixed-layer heat budget is analyzed. Mean surface westerlies along the ITCZ (5–10°S) in December–January–February (DJF) leads to an increased (decreased) evaporation in the westerly (easterly) phase of the intraseasonal oscillation (ISO), during which convection is also enhanced (suppressed). Thus the anomalous shortwave radiation, latent heat flux and entrainment effects are all in phase and produce strong SST signals. During June–July–August (JJA), mean easterlies prevail south of the equator. Anomalies of the shortwave radiation tend to be out of phase to those of the latent heat flux and ocean entrainment. This mutual cancellation leads to a weak SST response in boreal summer. The resultant SST tendency is further diminished by a deeper mixed layer in JJA compared to that in DJF. The strong intraseasonal SST response in boreal winter may exert a delayed feedback to the subsequent opposite phase of ISO, implying a two-way air-sea interaction scenario on the intraseasonal timescale.

Keywords: SST, ISO, shortwave radiation, latent heat flux, ocean entrainment

Citation: Li, T., F. Tam, X. Fu, et al., 2008: Causes of the intraseasonal SST variability in the tropical indian ocean, *Atmos. and Oceanic Sci. Lett.*, 1, ??-??.

1 Introduction

First discovered in the atmosphere (Madden and Julian 1971, 1972), the intraseasonal oscillation (ISO) also has strong signals in the ocean (e.g., Kindle and Thompson, 1989; Woolnough et al., 2000). Hendon and Glick (1997) reported a systematic relationship between sea surface temperature (SST) and large-scale convection associated with ISO in northern winter, and found that negative SST signals in general lag positive anomalies of convection by about 1/4 cycle. A one-dimensional mixed layer model of Shinoda and Hendon (1998) reproduced SST fluctuations similar to those observed during ISO events in boreal winter. Sengupta et al. (2001) showed that there is a similar phase relationship between the SST and convection for the boreal summer ISO. Using a 4½-layer ocean model, Waliser et al. (2003, 2004) examined the response of the tropical Indo-Pacific Oceans to composite ISO forcing, and noted that in addition to the surface heat fluxes, mixed layer dynamics and three-dimensional ocean processes also play a role in accurately representing the evolution of the SST. Using the Tropical Rainfall Measurement Mission (TRMM) Microwave Image (TMI) products, Saji et al. (2006) found that the strongest intraseasonal SST variability with a zonal elongated pattern appears in the southern Indian Ocean (5–10°S), where the climatological mean thermocline is shallow (Li et al., 2002).

Figure 1 illustrates the annual cycle of strength of the intraseasonal SST variability along 5–12.5°S. The longitude-time profile highlights the seasonal dependence of the intraseasonal SST anomaly (SSTA) over the southern Indian Ocean. The SSTA amplitude over this latitudinal band is strongest (weakest) during late boreal winter (summer). It is worth noticing that the change of the SSTA amplitude from boreal winter to summer reaches 40 %–50 % over the most part of the basin, despite the fact that the summer and winter ISO forcing have comparable amplitudes in the region.

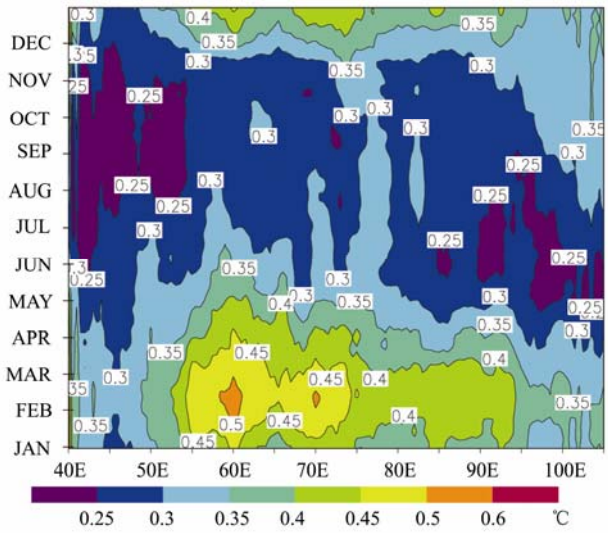

Figure 1 Standard deviation of the 25–90–day band-pass filtered SST averaged over 5–12.5°S, computed based on TMI data during the period of 1998–2005 (A 90–day moving window is applied throughout the calendar year).

Corresponding author: Tim Li, timli@hawaii.edu

The summer–winter contrast of the observed intraseasonal SST variability motivates us to investigate the cause of the season-dependent characteristic. The climatological thermocline dome over the southern Indian Ocean may explain the preferred location for the occurrence of the maximum SST variability, but it cannot explain the seasonal dependence feature as the thermocline dome appears all year around with a minor annual variation. In this study we intend to explore the cause of the strong seasonal-dependent intraseasonal SST variability, using an intermediate ocean model. The goal of the present study is to examine the role of different oceanic processes in determining the SST fluctuations during the passing of atmospheric ISO events, with a focus on how these processes and their inter-relationship depend on the seasonal cycle.

2 Data and model experiment

The main datasets are daily surface products from the ECMWF 40-year reanalysis (ERA-40) for the period of 1987–2001 (Uppala et al., 2005), daily TMI SST from 1998 to 2005, and ocean mixed-layer depth data from Laboratoire d'Océanographie Dynamique et de Climatologie.

A 2½-layer tropical ocean model (Wang et al., 1995; Fu and Wang, 2001) is used for the current study. The model has a $0.5^{o}\times0.5^{o}$ horizontal resolution. Vertically, it consists of two layers on top of an infinitely deep motionless ocean. The uppermost layer is the mixed layer, which exchanges mass with the second layer through entrainment and detrainment. The heat content of the mixed layer at each model grid point is determined by horizontal temperature advection, the difference between the net surface heat flux (Q_{net}) and the penetrated shortwave radiation (Q_{pet}), and cooling due to entrainment. Q_{net} is the sum of the surface shortwave radiation, longwave radiation, latent heat flux and sensible heat flux. Salinity effect is not included. For a detailed description of the model dynamics and physics, the readers are referred to Wang et al. (1995) and Fu and Wang (2001).

The model was spun up from the rest with a 10-year integration based on the climatological annual cycle forcing. Then the model is forced by ERA-40 daily reanalysis products, which include winds at 10 m, net longwave and shortwave radiation at the surface, and 2 m air temperature for the period of 1987–2001. A bulk formula is used to calculate the surface latent heat flux, with the surface specific humidity q_a being related to the model SST according to an empirical relation: $q_a=(0.972\times SST-8.92)\times10^{-3}$ (Wang et al., 1995). To mimic the high-frequency wind effect, a minimum wind speed of 4 m s^{-1} is imposed within 5^{o}N–5^{o}S when the heat flux is calculated. Pentad mean model outputs are archived for further analyses.

3 Simulation results and mixed-layer heat budget analyses

Figure 2 plots the standard deviation of the model 25–90-day band-pass filtered SST fields in December–January–February (DJF) and June–July–August (JJA). During boreal winter, a zonally elongated band of strong intraseasonal SST responses can be found along 10^{o}S, with the maximum amplitude of about 0.3 ^{o}C. In contrast, such a feature is completely absent in boreal summer simulations. Instead, the strongest SST response occurs in the northern part of the Arabian Sea and the Bay of Bengal, and also over the equatorial eastern Indian Ocean. In general, the features of the simulated SST variability are consistent with where the strongest intraseasonal activity of the zonal wind and Outgoing Longwave Radiation (OLR) is located. The seasonal contrast of the intraseasonal SST variability from the model simulation agrees well with the observed, even though the overall strength of the simulated intraseasonal SST variability is a little weaker over the southern Indian Ocean, due to the relatively weak wind forcing (compared to the QuikSCAT product) and the overestimation of the mixed layer depth in the model.

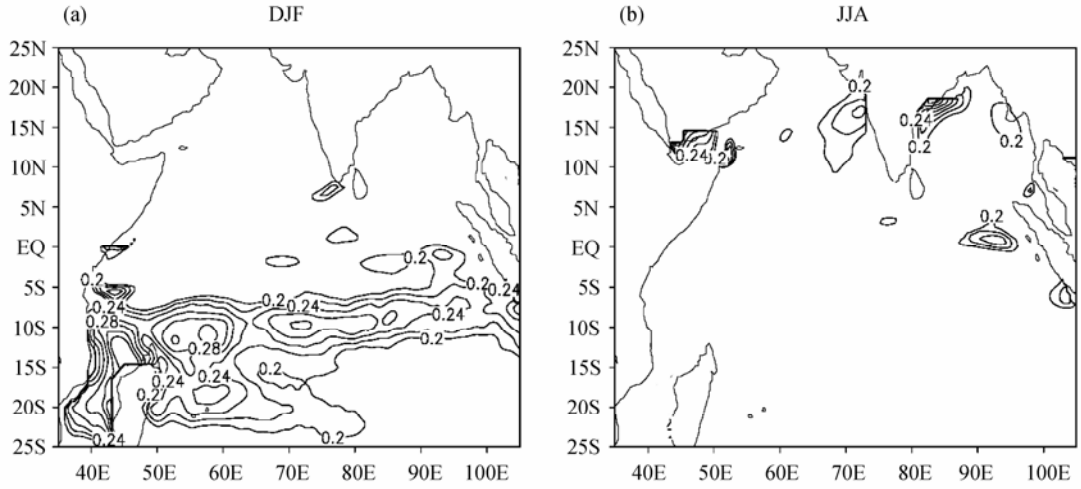

Figure 2 The standard deviation patterns of the simulated 25–90-day band-pass filtered SST during (a) DJF and (b) JJA. Contour interval is 0.02 ^{o}C, starting from 0.2 ^{o}C.

Given that the model is capable of simulating the winter-summer asymmetry of the intraseasonal SST variability, we further investigate specific processes that give rise to the asymmetry. Figure 3 shows the evolution of the model SSTA, along with wind stress and OLR anomalies, during a composite ISO cycle over the Indian Ocean for the DJF (left panels) and JJA (right panels) seasons. The time series of the 25–90-day band-pass filtered zonal wind stress, averaged over the domain of 5–12.5°S, 50–65°E, is chosen as an index to characterize the ISO cycle during DJF. For the JJA season, the wind stress averaged over 2.5–10°S, 75–90°E is used. In Fig. 3, the SST, wind stress and OLR signals are all regressed onto the ISO indices. First, we discuss the evolution of the SSTA in DJF. In pentad −1 (figure not shown), westerly wind stress and negative OLR signals associated with an active phase of ISO appear in the tropical Indian Ocean. Cold SSTA at about 10°S, 55°E appears in pentad 0 (Fig. 3a). Since the background wind is westerly in the vicinity of this latitude, a positive zonal wind stress anomaly increases the evaporative cooling in the region. This gives rise to the in-phase relationship between the anomalous surface shortwave radiation and the latent heat flux, and together they act with the ocean entrainment to strongly cool the model SST at this phase of the ISO. As a result, in pentad +1, the cold SSTA is enhanced over the western to central Indian Ocean along ~ 10°S (see Fig. 3b). One pentad later (Fig. 3c), signals of suppressed convection appear at about 55°E, collocated with the cold SST response. The positive OLR anomaly subsequently expands eastward and grows (Fig. 3e). It is noteworthy that suppressed convection tends to develop over the location where cold SST is already present for five to ten days, as inferred from the sequence of charts from pentad +1 to +3. This phase relationship between the SST and convection implies a delayed two-way air-sea interaction scenario for the ISO, this is, on the one hand, an ocean cooling is induced by the wet (westerly) phase of the ISO through combined cloud radiative forcing and surface evaporation/ocean vertical mixing, and on the other hand, the so-induced western Indian Ocean cold SSTA in turn initiates a subsequent dry (easterly) phase of the ISO. Thus, air-sea interactions may play a role in the re-initiation of the ISO over the western Indian Ocean during boreal winter.

Next, we examine the evolution of the wind stress, convection and SST associated with ISO in boreal summer. In pentad −2 (figure not shown), enhanced convection first appears over the eastern equatorial Indian Ocean. This is followed by further development of convection and the appearance of surface westerlies one pentad later. In pentad 0 when the westerlies are still strong, the maximum convection anomaly starts to propagate northward to the Bay of Bengal (Fig. 3b). In the next three pentads (Figs. 3d, 3f, and 3h), suppressed convective anomalies gradually move eastward, as easterly wind stress anomalies replace the original westerly wind stress anomalies in the eastern Indian Ocean. This picture of summertime ISO evolution is consistent with the one portrayed by Kemball-Cook and Wang (2001), Fu et al. (2003), and Jiang and Li (2005).

The overall SST response in boreal summer is much weaker than that in boreal winter, even though the wind stress and convection perturbations associated with the ISO have comparable amplitudes. To demonstrate the relative role of the ocean dynamics and heat flux processes in causing the seasonal asymmetric response, a mixed layer heat budget analysis is performed. Figure 4 shows the regressed SST tendency terms associated with the anomalous shortwave radiation, latent heat flux, entrainment cooling, and horizontal advection, respectively. They are regressed based on the same ISO indices defined previously, averaged over the lag of pentad −1 to pentad 0.

In boreal winter during the westerly phase of the ISO, enhanced convection across the basin causes SST cooling due to reduced shortwave radiation (Fig. 4a). At the same time, the wind anomalies reinforce the background wind, leading to stronger total wind speed and thus stronger surface evaporation and ocean entrainment/vertical mixing. The in-phase relationship between the two major heat flux terms and the entrainment results in a strong cooling tendency near 10° S in boreal winter (Figs. 4a, 4c, and 4e), while the SST tendency due to horizontal advection is weak (Fig. 4g). Therefore, the background mean flow plays an important role in producing a strong SST tendency associated with the passing of the ISO in DJF over the southern Indian Ocean.

During boreal summer, the phase relationship between various tendency terms is markedly different from that in winter. Westerly wind anomalies over the southeastern Indian Ocean produce a warming effect along 5-10°S (Figs. 4d and 4f). This is because, during JJA, the mean surface wind is easterly south of the equator, implying the reduction of the total wind speed and hence less evaporation and entrainment. On the other hand, enhanced convection leads to SST cooling due to decreased shortwave radiation (Fig. 4b). Thus the shortwave cooling is opposing the anomalous warming due to the evaporation and entrainment. Furthermore, anomalous horizontal temperature advection opposes the latent heat and entrainment effect along 5°S (Fig. 4h). This is because the westerly wind stress causes eastward and northward surface currents that advect cold water from both the west and the south, leading to a cooling tendency over the region. The mutual cancellation among the tendency terms leads to a weak SST response in JJA over the region.

The annual variation of the mixed layer depth (MLD) is an additional factor that enhances the summer–winter SST asymmetry. Both the observed and simulated MLDs attain a minimum (maximum) during December–March (August–September). The magnitude of the mean MLD in boreal summer is about twice as large as that in boreal winter. This implies that even given the same anomalous heat flux forcing, the SST variability could be smaller (greater) in boreal summer (winter) due to the deeper (shallower) mixed layer.

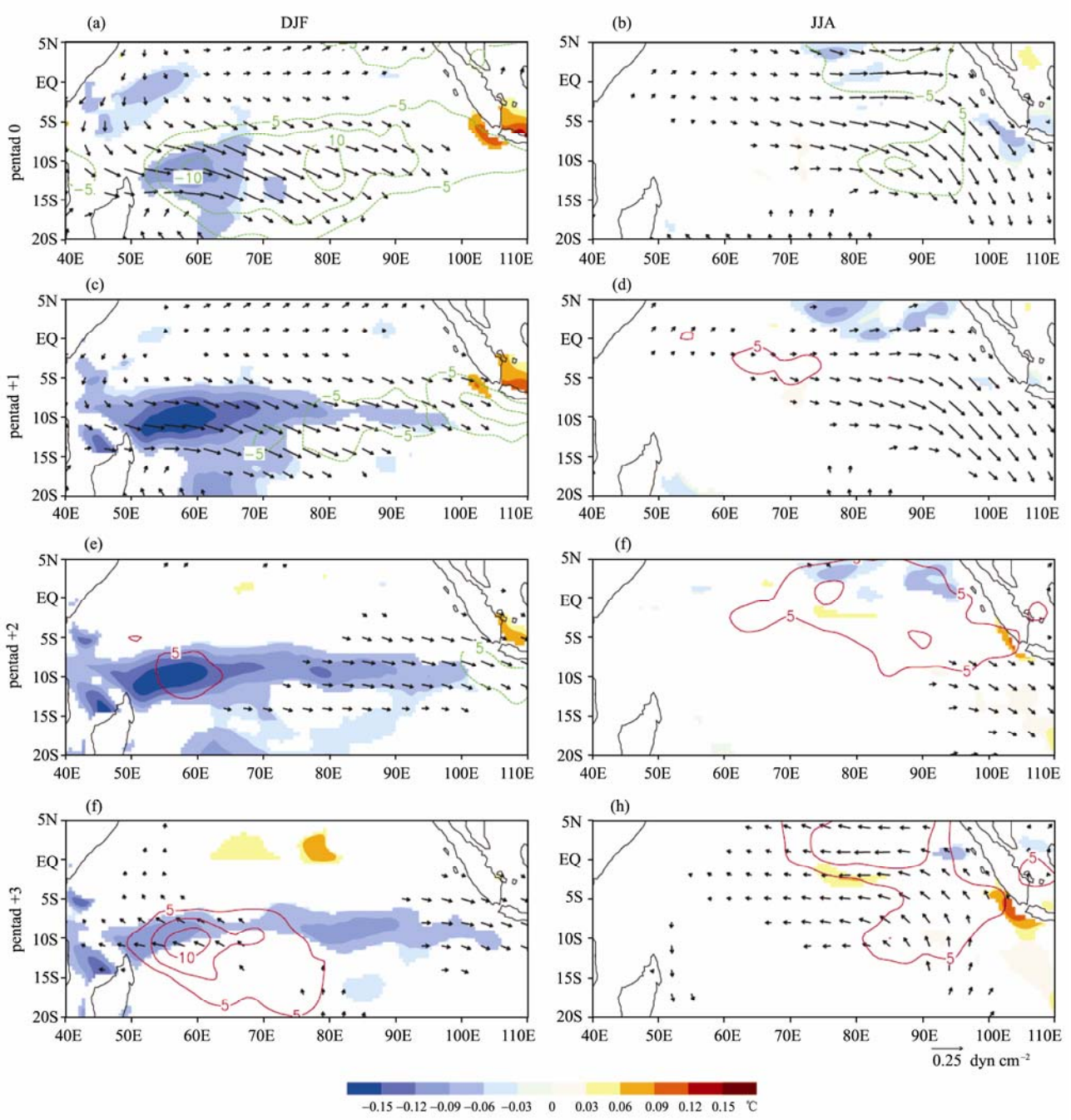

Figure 3 Regression coefficients of the simulated SSTA (shading) and observed wind stress (arrow) and OLR (red contours for positive and green contours for negative values, starting from ± 5 W m^{-2}, interval: 2.5 W m^{-2}) anomalies for the lag of (a and b) 0, (c and d) +1, (e and f) +2, and (g and h) +3 pentads, based on data from the DJF (left panels) and JJA (right panels) periods. Wind stress and SST (OLR) anomalies being shown are above the 95 % (90 %) significance level.

4 Conclusion and discussion

Observations show a striking asymmetry between the summer and winter intraseasonal SST variability. In boreal winter, the strongest SST anomalies are found over the latitudinal band of 5–10°S. In boreal summer, SST signals are almost absent south of the equator. To study the cause of the SST asymmetry, a 2½-layer ocean model was used, and the model was forced by daily ERA-40 reanalysis products. In general, the model simulations capture well the seasonal contrast of the SST response to the ISO forcing, even though the amplitude is a little weaker compared to the satellite observation.

Based on a heat budget analysis, the winter-summer asymmetry of the SST response over the southern Indian Ocean may be understood as follows. During DJF, mean surface westerlies prevail along the ITCZ (5–10°S) across the Indian Ocean basin. When the ISO surface wind is westerly (easterly), enhanced (reduced) evaporative cool-

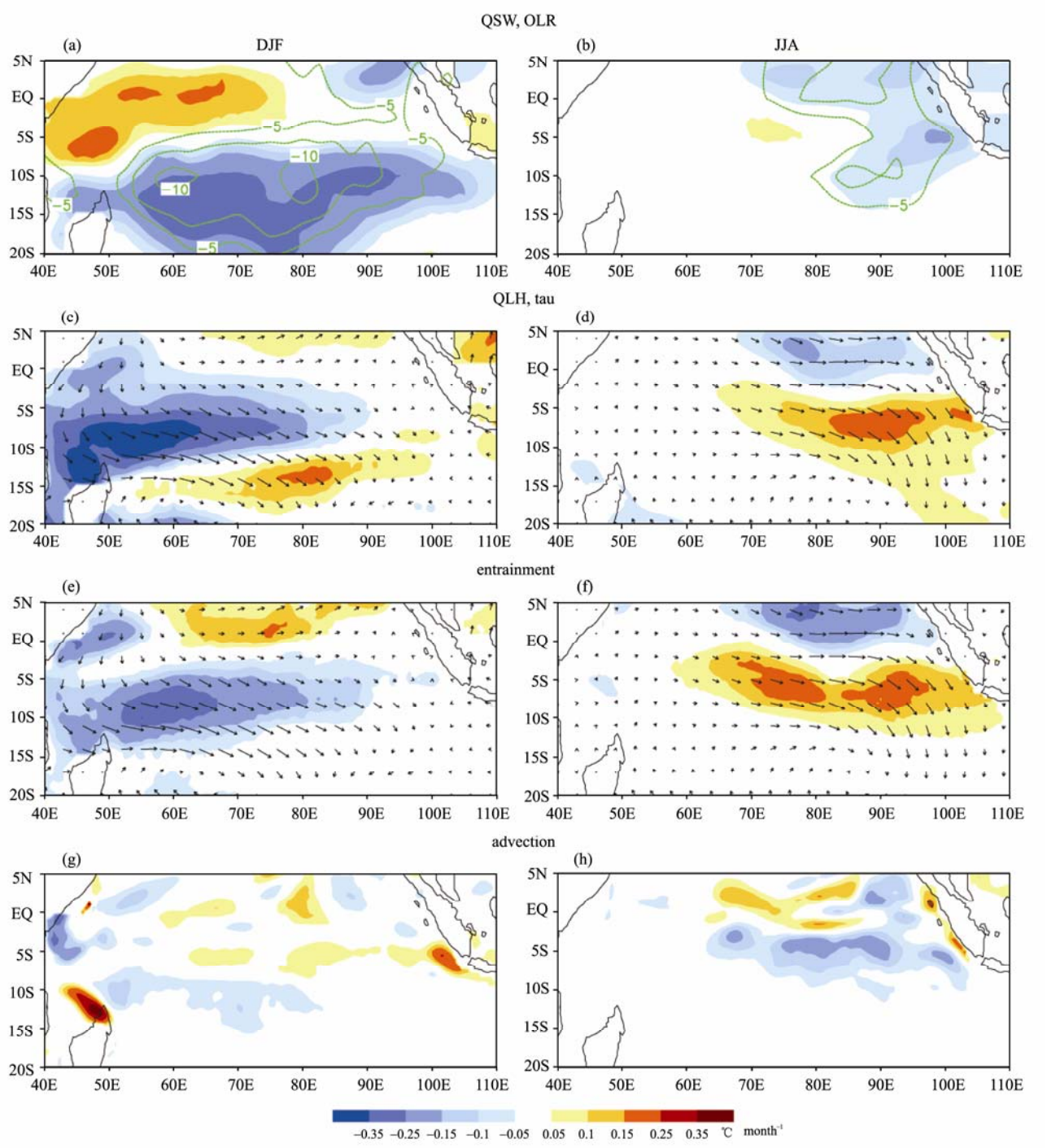

Figure 4 Anomalies of (a and b) the net shortwave radiation (shading) and OLR (contour, interval: 2.5 W m^{-2}), (c and d) the surface latent heat flux (shading) and wind stress (arrow), (e and f) temperature tendency due to ocean entrainment (shading) and wind stress (arrows), and (g and h) horizontal temperature advection in DJF (left panels) and JJA (right panels). See scale bar at bottom for SST tendency terms. Here the shortwave radiation and latent heat flux terms have been divided by the climatological mean mixed layer depth and water density and specific heat to reflect the same temperature tendency units as the entrainment and advection terms.

ing results. Combined with the fact that the ISO westerly is nearly in phase with convection, the latent heat flux and shortwave radiation anomalies therefore tend to be in phase. Anomalies of entrainment and the latent heat flux also have the same sign. These three ISO forcing terms, having comparable magnitudes, act together to produce strong SST responses over the southern Indian Ocean in boreal winter. During JJA, the mean surface wind becomes easterly in the same region. This makes the anomalous incoming shortwave radiation against the latent heat flux and ocean entrainment. Meanwhile, there is negative horizontal temperature advection just south of the equator, due to the northward Ekman drift during the westerly phase of the ISO. Thus there is mutual cancella-

tion among the temperature tendency terms. As a result, the SST response is weak in boreal summer. This seasonal asymmetry of the SST response is further amplified by the annual cycle of the MLD, which is shallower (deeper) in the boreal winter (summer).

A number of mechanisms have been proposed to explain the re-initiation of the ISO. Most of them, however, involve the atmospheric processes (e.g., Matthews, 2000; Seo and Kim, 2003; Jiang and Li, 2005). In our simulations, significant SST anomalies are found over the western Indian Ocean in boreal winter after the passing of the ISO. Because of its strong amplitude, the SSTA may help initiate an opposite phase of the ISO in the western Indian Ocean. In contrast, the SST signal associated with the summer ISO is weak. Thus, it is less likely that air-sea interactions play a role in the re-initiation of the ISO in boreal summer.

Acknowledgments. This work was supported by the National Natural Science Foundation of China Grants 40628006 and 40675054. Tim Li was also supported by ONR grants N000140710145, N00173061G031 and N000140810256 and by the International Pacific Research Center that is sponsored by the Japan Agency for Marine-Earth Science and Technology (JAMSTEC), NASA (NNX07AG53G) and NOAA (NA17RJ1230). This is SOEST contribution number 7508 and IPRC contribution number 537.

References

Fu, X., and B. Wang, 2001: A coupled modeling study of the seasonal cycle of the Pacific cold tongue. Part I: Simulation and sensitivity experiments, *J. Climate*, **14**, 765–779.

Fu, X., B. Wang, T. Li, et al., 2003: Coupling between northward-propagating, intraseasonal oscillations and sea surface temperature in the Indian Ocean**,** *J. Atmos. Sci.*, **60**, 1733–1753.

Hendon, H. H., and J. Glick, 1997: Intraseasonal air–sea interaction in the tropical Indian and Pacific Oceans, *J. Climate*, **10**, 647–661.

Jiang, X., and T. Li, 2005: Re-initiation of the boreal summer intraseasonal oscillation in the tropical Indian Ocean, *J. Climate*, **18**, 3777–3795.

Kemball-Cook, S. R., and B. Wang, 2001: Equatorial waves and air–sea interaction in the boreal summer intraseasonal oscillation, *J. Climate*, **14**, 2923–2942.

Kindle, J. C., and J. D. Thompson, 1989: The 26- and 50-day oscillations in the western Indian Ocean: Model results, *J. Geophys. Res.*, **94(**C4**)**, 4721-4736, doi:10.1029/88JC04300.

Li, T., Y. S. Zhang, E. Lu, et al., 2002: Relative role of dynamic and thermodynamic processes in the development of the Indian Ocean dipole, *Geophys. Res. Lett*., **29**, 2110–2113.

Madden, R. A., and P. R. Julian, 1971: Detection of a 40-50 day oscillation in the zonal wind in the tropical Pacific, *J. Atmos. Sci.*, **28**, 702–708.

Madden, R. A., and P. R. Julian, 1972: Description of global-scale circulation cells in the tropics with a 40−50 day period, *J. Atmos. Sci.*, **29**, 1109–1123.

Matthews, A. J., 2000: Propagation mechanisms for the Madden-Julian oscillation, *Quart. J. Roy. Meteor. Soc.*, **126**, 814−837.

Saji, N. H., S.-P. Xie, and C.-Y. Tam, 2006: Satellite observations of intense intraseasonal cooling events in the tropical South Indian Ocean, *Geophys. Res. Lett.*, **33**, L14704, doi: 10.1029/2006GL026525.

Sengupta, D., B. N. Goswami, and R. Senan, 2001: Coherent intraseasonal oscillations of ocean and atmosphere during the Asian summer monsoon, *Geophys. Res. Lett.*, **28(**21**)**, 4127–4130, doi:10.1029/2001GL013587.

Seo, K. H., and K. Y. Kim, 2003: Propagation and initiation mechanisms of the Madden-Julian oscillation, *J. Geophys. Res.*, **108(**D13**)**, 4384–4405.

Shinoda, T., and H. H. Hendon, 1998: Mixed layer modeling of intraseasonal variability in the tropical western Pacific and Indian Oceans, *J. Climate*, **11**, 2668–2685.

Uppala, S. M., P. W. KÅLLBERG, A. J. SIMMONS, et al., 2005: The ERA-40 re-analysis, *Quart. J. Roy. Meteor. Soc.*, **131**, 2961–3012.

Waliser, D. E., R. Murtugudde, and L. E. Lucas, 2003: Indo-Pacific Ocean response to atmospheric intraseasonal variability: 1. Austral summer and the Madden-Julian oscillation, *J. Geophys. Res.*, **108(**C5**)**, 3160, doi:10.1029/2002JC001620.

Waliser, D. E., R. Murtugudde, and L. E. Lucas, 2004: Indo-Pacific Ocean response to atmospheric intraseasonal variability: 2. Boreal summer and the intraseasonal oscillation, *J. Geophys. Res.*, **109**, C03030, doi:10.1029/2003JC002002.

Wang, B., T. Li, and P. Chang, 1995: An intermediate model of the tropical Pacific Ocean, *J. Phys. Oceanogr.*, **25**, 1599–1616.

Woolnough, S. J., J. M. Slingo, and B. J. Hoskins, 2000: The relationship between convection and sea surface temperature on intraseasonal timescales, *J. Climate*, **13**, 2086–2104.